Remote sensing dynamic monitoring of eco-water (layer) conservation spatiotemporal variation in earthquake stricken areas

Mingshun Xiang[a,*], Jin Yang[a], Wunian Yang[b,c], Chunjian Wang[a,b], Linsen Duan[a]

[a]*College of Tourism and Urban-Rural Planning, Chengdu University of Technology, Chengdu 610059, China,*
email: xiangmingshun19@cdut.edu.cn
[b]*College of Earth Science, Chengdu University of Technology, Chengdu 610059, China*
[c]*Key Laboratory of Geoscience Spatial Information Technology of Ministry of Land and Resources,*
Chengdu University of Technology, Chengdu 610059, China

ABSTRACT

Water is the major guarantee for ecological restoration and a virtuous ecological cycle. This study is based on spatial information processing technology and mathematical modeling. The results demonstrate that the overall trend in regional modulus of eco-water conservation (MEC) and quantity of eco-water conservation (QEC) was dropped dramatically and then gradually increased from 2007 to 2017. The restoration process of eco-water conservation capacity cannot match both in time and space. Moreover, there are significant differences in MEC between different land types. Serious destruction of forestland are the leading factors of the 14.27% decrease in MEC of the study area after earthquake. Besides, there is an apparently positive correlation between MEC distribution and slope changes on the whole ($p < 0.05$), so the earthquake has the greatest impact on MEC if the surface slope is between 15° and 35°. Furthermore, the average MEC in areas below 3,000 m above sea level is higher than in other areas, and the MEC reduction rate after the earthquake is 31.85% higher than the areas above 3,000 m. In addition, the disturbance of MEC around faults was more often than that in other areas.

Keywords: Eco-water (layer); Remote sensing inversion model; Wenchuan earthquake; Ecological restoration; Dynamic change

1. Introduction

Eco-water (layer), a new concept put forward by research groups from the perspective of eco-hydrology in recent years, which refers to the water body closely related with plants on the surface of the earth. It is a layer after the transformation of atmospheric precipitation and stored by vegetation, vegetation humus layer, and root soil layer, in other words, eco-water layer which centered around vegetation [1]. Eco-water (layer) is essentially different from terms like ecological water, ecological water demand, and ecological environment water demand in common documents. It's the water body closely related with plants on

the surface of the earth and a key storage water body in the surface of the terrestrial ecological environment. It has the function of buffer, distribution, and regulation for precipitation and plays an important role in the improvement of ecological environment and hydrological cycle. Besides, eco-water (layer) is the center of determining the dynamic distribution of water resources, it also has noticeable specificity and complexity in the whole hydrological cycle system. It is of great scientific significance to study and accurately quantify the eco-water (layer) of land vegetation for the entire water environment research [2,3].

The vegetation, soil, and water were severely damaged in Wenchuan earthquake in May 12, 2008, which

* Corresponding author.

changed the original ecological process of the vegetation and hydrology in this area and deteriorated the basic conditions for vegetation growth and development, leading to ecological vulnerability, and landscape fragmentation [4–6]. Moreover, the earthquake and its secondary geological disasters destroyed the underground confining bed, changed the geological condition and hydrological process, reduced water and fertilizer storage capacity of the soil and resource utilization efficiency of water, and then threaten the stability and security of regional ecosystem [7]. As a crucial factor for vegetation ecology restoration in earthquake stricken areas, water, the source of human survival and development, plays a significant part in regulating the ecological environment and hydrologic cycle. At the same time, as an important indicator to measure the quality of ecological environment, water conservation capacity plays an essential role in regional and global ecosystem stability [8,9]. Therefore, water ecological environment and its spatiotemporal changes in earthquake stricken areas should be explored in a profound and accurate way, and corresponding protection measures should be proposed. They are full of great importance for the scientific management of the ecological environment in the earthquake stricken areas and the formulation of long-term ecological restoration.

The water environment has remarkable diversity and complexity in the huge terrestrial ecosystem, so researchers try to study on the separation of water resources from groundwater, soil water, and surface water according to the characteristics of time and space, movement, and storage of water. In particular, they separated "green water" from other water resources from the perspective of ecological water demand, and this caused the scientific community to rethink the concept of water resources and hydrological functions [10]. In recent years, hydrologists have used hydrological methods as the basis and many new technologies like remote sensing (RS) and geographic information system (GIS) to carry out researches on many issues around the world as the combination. The issues involved distributed hydrological cycle model [11–14], estimation, and variation analysis of water reserves [15–17], simulation of water–soil–vegetation–atmosphere transmission system [18–20], remote sensing hydrological coupling model [21–23]. These methods provide a scientific basis for researches on water resource in stricken areas. Based on these researches, relevant scholars analyzed the changes of surface hydrology [24,25], water quality [26–28], and underground water [29–31] in earthquake stricken areas, which provided scientific bases for forecast assessment and integrated management of water resources.

The existing research results have apparent advantages in the quantitative analysis of groundwater, surface water, soil water, and vegetation water. But Wenchuan earthquake stricken area is a place with complex geology and landform, conventional approaches are difficult to meet the needs of accurate eco-water quantification and dynamic monitoring on the surface. Researches on the spatiotemporal change features and quantitative analysis of land surface vegetation eco-water (layer) in the severely earthquake stricken area are still in the blank stage. Recently, the coupling model of remote sensing hydrology is a significant direction with broad prospects for the development of water resources

prediction mode [32–34]. The practice of research groups in recent years shows that using remote sensing technology to study the eco-water (layer) in Western Sichuan Plateau and earthquake stricken areas with poor environment is desirable on theoretically and technically [1–3,35].

Thus, based on the previous research results of the research group and 3S technology (RS, GIS, and GNSS), this paper constructs a quantitative inversion model of eco-water (layer) due to the lack of ecological water research in Wenchuan earthquake stricken areas. The dynamic monitoring of eco-water (layer) conservation by remote sensing during 10 y before and after the earthquake in the study area revealed the distribution structure and spatiotemporal variation features of eco-water (layer) in earthquake stricken areas, enriched the theoretical system of ecological recovery research in earthquake stricken areas, and provided a theoretical basis for the promotion of the ecological restoration process and the optimization of restoration measures in this area.

This paper is organized as following. The first part is a review of the research status of hydrological remote sensing and a description of the significance of eco-water (layer) remote sensing dynamic monitoring for ecological restoration in earthquake stricken areas. The second part presents the research region status, research data acquisition, and processing procedure, eco-water (layer) remote sensing inversion method, and model. The third part includes the analysis of characteristics of inter-annual and spatial changes of eco-water (layer) conservation in the research area, the study of the impact of earthquake on regional eco-water (layer) conservation capacity, and the discussion of spatiotemporal differences of eco-water conservation capacity. The last part discusses and summarizes the study.

2. Materials and methods

2.1. Study area

Beichuan, a county in the northwest part of Sichuan Province, is located at 103°44'42.41"E to 104°43'15.37"E and 31°33'35.63"N to 32°13'10.97"N, covering an area of 3,083.30 km², shown in Fig. 1.

Most parts of the county are dominated by mountains with an elevation of 540–4,769 m. Generally speaking, the terrain is high in the northwest and low in the southeast. With intense tectonic movement and complex underlying lithology and geological structure, the main part of Longmen Mountain fault zone (from Beichuan County to Yingxiu Town) is one of the areas with the strongest seismic activity and of highest frequency. Soil and vegetation are characterized by vertical distribution. From high altitude to low altitude, the distribution of vegetations are from alpine screes vegetation, alpine meadow, sub-alpine shrub meadow, coniferous forest, coniferous and broad-leaved mixed forest, evergreen deciduous broad-leaved mixed forest to subtropical evergreen broad-leaved forest. The soils are from alpine cold desert soil, alpine meadow soil, sub-alpine meadow soil, brown soil, dark brown soil, and yellow–brown soil to yellow soil. As an important water conservation area in Chengdu Plain, the study area is of great importance to China's ecological shelters and biodiversity
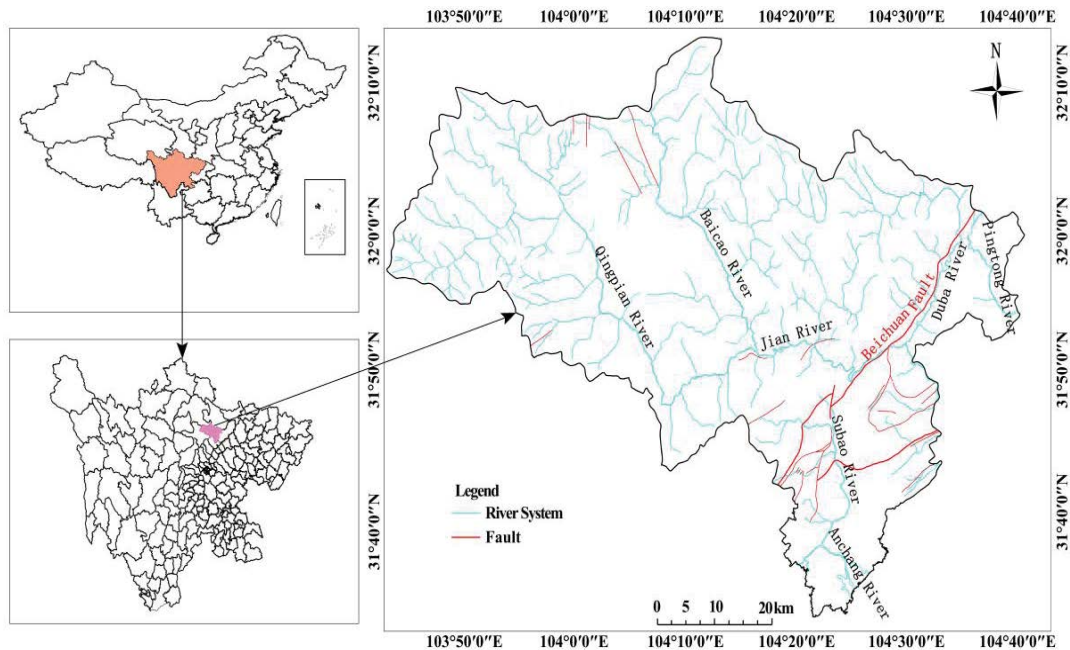
Fig. 1. Location of the study area.

protection zones. Due to the Wenchuan earthquake and its secondary geological disasters, the vegetation coverage has declined significantly; the landscape fragmentation has intensified; water has been seriously damaged; the ecological carrying capacity has declined; the biodiversity has been threatened, and the ecological service function has been seriously degraded in this area. Restricted by many factors, the ecological recovery after earthquake is quite long and difficult, so long-term dynamic monitoring and evaluation on ecological environment should be done.

2.2. Datasets

2.2.1. Remote sensing data

The thesis is divided into five parts according to time, 2007 (pre-earthquake), 2008 (earthquake year), 2011 (early recovery), 2014 (recovery mid-term), and 2017 (recovered mid-to-late term). Remotely sensed Landsat time series images from Landsat 5 TM images (acquired on 18 July 2008; 05 August 2011), Landsat 7 ETM+ images (acquired on 19 September 2007), and Landsat 8 OLI images (acquired on 12 July 2014; 06 September 2017). The 2007–2017 dataset was at 30 m spatial resolution. The data from the US Geological Survey (USGS) at http://glovis.usgs.gov/. Image processing is done in eight main steps: radiometric calibration, atmospheric correction, removing striping, image fusion, projection transformation, image registration, image mosaic, and image cutting.

ASTER digital elevation model (DEM) with spatial resolution of 30 m. DEM data from the geological data cloud at http://www.gscloud.cn/. Image processing is done in eight main steps: coordinates correction, eliminate noise, image mosaic, and image cutting.

The data of land use classification comes from China's second land survey results data set.

2.2.2. Sample collection and processing

Soil and vegetation samples were collected from different places and types in the study area, including 118 soil samples and 103 vegetation samples. Soil samples were collected by cutting rings with a diameter of 50.46 mm, height of 50 mm, and volume of 100 cm^3. Each sample was weighed and numbered. The latitude and longitude coordinates of each sample were recorded, respectively. Then soil samples were weighed one by one through an analytical balance with a precision of 0.0001 g. Sample was weighed three times and the average of the results was taken. Next, these samples were put in an oven at 105°C and dried continuously for more than 72 h until they reached a constant weight. The unit of soil water content is expressed by the thickness of soil water layer (W_c) in g/cm^2.

$$W_c = H \times \frac{G_1 - G_2}{G_2} \times \rho \tag{1}$$

The internal height of the cutting ring used in this paper is 5 cm. In Eq. (1), H refers to the overall soil layer thickness used for calculation; G_1 is the soil quality in wet; G_2 is the soil quality after drying; ρ is the soil bulk density.

Representative canopy leaf samples were selected at each sampling site, and 3–5 plants of each type were taken. After sampling, these samples were weighed immediately, then they were sealed in the sample bags and marked with their number and coordinate. Then plant samples were baked in a 70°C oven for about 24 h in the laboratory until they reached a constant weight. The unit of vegetation water content is expressed by equivalent water layer thickness (EWT) in g/cm^2.

$$EWT = \frac{FW - DW}{A} \times 100\% \tag{2}$$

In Eq. (2), EWT refers to the content of water per unit area; FW is the fresh weight of vegetation, DW is the dry weight of vegetation; *A* represents the leaf area.

ASD FieldSpec Pro FR (measuring range 350–2,500 nm) was used to collect spectral data of the soil and vegetation. As the spectrometer was exposed to environmental factors, the spectral reflectance of soil and leaf may have some error. Therefore, respective values were corrected using a standard whiteboard. The reflectance was measured thrice and values recorded three times each using a spectrometer for each measurement.

2.3. Methods

2.3.1. Remote sensing inversion method of soil water content

In the paper, Nir-Red eigenspace method was used to carry out the remote sensing inversion in soil water content. Some scholars believe that Nir-Red spectral feature space image is referring to typical triangle distribution which is shown in Fig. 2 [36–39].

In Fig. 2, the straight line formed by *B* and *C* is the soil line. The soil from point *B* to *C* was changed from wet to dry. The regression equation of *B–C* as the soil baseline can be gotten through the two-dimensional spectral point fitting. Eq. (3) is as follows:

$$R_{nir} = MR_{red} + I \tag{3}$$

In Eq. (3), R_{nir} refers to the reflectivity of near-infrared band; R_{red} is the reflectivity of red band; *M* is the slope of soil line; *I* is the intercept of soil line in the ordinate.

In Fig. 2, *L* is the line perpendicular to the soil baseline through the origin of coordinates, the calculation equation of *L* is:

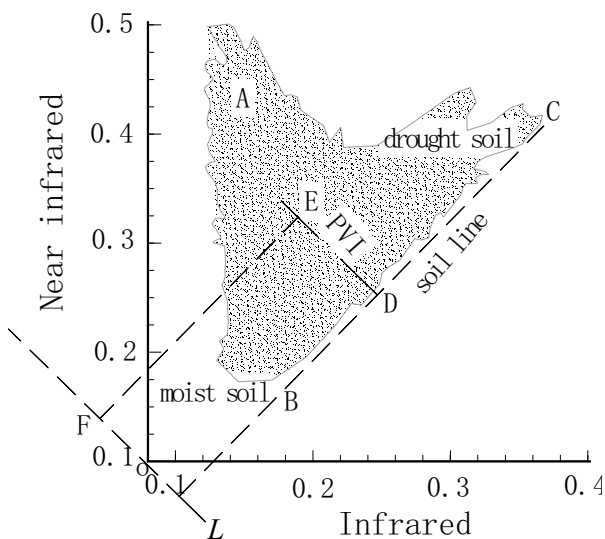$$R_{nir} = -\frac{1}{M} R_{red} \tag{4}$$

Fig. 2. Schematic diagram of soil moisture monitoring model.

In Nir-Red two-dimensional feature space, the vertical distance from any point to line *L* reflects the drought degree of surface soil. The larger the distance is, the drier the surface soil is. Otherwise, the wetter the surface soil is. The equation is as follows:

$$EF = \frac{1}{\sqrt{M^2 + 1}} \left(R_{red} + MR_{nir} \right) \tag{5}$$

When the soil is dry, the soil water content is very low or even zero, then the EF is infinitely close to 1. When the soil water content is extremely high, the soil water content reaches 100%, then the EF will approach 0 infinitely. Based on this relationship, the constant 1 is introduced to subtract the EF value. The equation for prediction model of soil water content in Nir-Red two-dimensional feature space is as follows.

$$SMMRS = 1 - \frac{1}{\sqrt{M^2 + 1}} \left(R_{red} + MR_{nir} \right) \tag{6}$$

According to Eq. (6), the slope of soil line needs to be determined to calculate SMMRS. Qin et al. [42] found that the soil line extracted from the two-dimensional spectral feature space constituted by infrared and near-infrared bands based on remote sensing images met the linear relationship, and this was verified by field measurement in different regions [39].

The measured thickness of soil water layer and SMMRS linear fitting model were established to estimate the soil water content in the study area [Eq. (5)]:

$$W_c = a \times SMMRS + b \tag{7}$$

2.3.2. Remote sensing inversion method of vegetation water content

As the change of vegetation water content, its spectral characteristics will change accordingly. Relevant studies have found that the response of vegetation water content at 820; 860; 900; 950; 1,240; and 1,600 nm is relatively high, so it is more accurate to estimate vegetation canopy water content by establishing a relationship model between vegetation index and measured vegetation water content [3,40,41]. The correlation between vegetation index (like MSI, SR, SRWI, OSAVI, etc.) and canopy water content was calculated in turn, and the relevant data is shown in Table 1. According to the previous findings of the research group, the moisture stress index (MSI) was selected for study [3,35,42].

Eq. (6) established the vegetation water content measured system and MSI linear fitting model to estimate the vegetation water content in the study area:

$$EWT_c = a \times MSI + b \tag{8}$$

2.3.3. Inversion method of eco-water (layer)

According to the definition of MEC, the eco-water conservation modulus model ($MEC(i,j)_t$) in pixel (*i,j*) at time *t* is:

Table 1
Common vegetation index and equation

Vegetation index	Linear regression model	r	RMSE
$SR = R_{895}/R_{675}$	$y_1 = 0.0122x + 0.6114$	0.730	0.0287
$NDII = (R_{820} - R_{1600})/(R_{820} + R_{1600})$	$y_2 = 0.6655x + 0.5243$	0.828	0.0272
$SAVI = 1.5 \times (R_{NIR} - R_{Red})/(R_{NIR} + R_{Red} + 0.5)$	$y_3 = 0.2181x + 0.6105$	0.471	0.0327
$MSI = R_{1600}/R_{820}$	$y_4 = -0.4421x + 0.9615$	0.871	0.0250
$MSAVI = 0.5 \times [2 \times R_{NIR} + 1 - ((2R_{NIR} + 1)^2 - 8(R_{NIR} - R_{Red}))^{0.5}]$	$y_5 = 0.2776x + 0.5756$	0.754	0.0282
$OSAVI = 1.16 \times (R_{800} - R_{670})/(R_{800} + R_{670} + 0.16)$	$y_6 = 0.2739x + 0.5588$	0.528	0.0333
$NDVI = (R_{895} - R_{675})/(R_{895} + R_{675})$	$y_7 = 0.2614x + 0.4933$	0.815	0.0273
$NMDI = [R_{860} - (R_{1640} - R_{2130})]/[R_{860} + (R_{1640} - R_{2130})]$	$y_8 = 0.7944x + 0.2154$	0.624	0.0320

$$MEC(i,j)_t = EWT_C(i,j)_t + W_c(i,j)_t \tag{9}$$

The QEC of the whole area is:

$$QEC = \sum_{i=1}^{m}\sum_{j=1}^{n} MEC(i,j)_t \times A(i,j)_t \tag{10}$$

The $A(i,j)_t$ refers to the area of pixel (i,j) at time t.

3. Results and analysis

3.1. Remote sensing inversion results of eco-water (layer) conservation in stricken areas

Linear regression models of W_c and EWT_c were established based on Eqs. (1)–(8) and Table 1, and the correlation coefficient (r) and root mean square standard error (RMSE) between measured results and predicted results of the model were used as effective indexes of the evaluation model. The fitting model and its prediction results are shown in Table 2.

High prediction accuracy of these two prediction models was observed. At last, the MEC of each time sequence in the study area is estimated by remote sensing according to Eq. (7), shown in Fig. 3.

3.2. Analysis on annual changes of eco-water (layer) conservation

From Fig. 3, we can see that the MEC spatial distribution characteristics in the study area are basically similar every year. Areas with high eco-water conservation capacity are mainly distributed in Jian, Duba, and Baicao river basin. The middle and western edges of the study area, while areas with low conservation capacity are mainly distributed in the south, north-central parts, and central areas of

counties and towns. From the perspective of changes in the spatial distribution of MEC, earthquake, and its secondary geological disasters have the greatest impact on the eastern part of the study area and the smallest impact on the western part of the study area, so the MEC changes are highly spatially coupled with regional damage. In 2011, the MEC in the eastern part of the study area was obviously higher than that in 2008, but the change in other parts of the study area was not evident. In 2014, the spatial distribution of MEC in the study area was more even, and the central and western part had a certain increase compared with 2011. During the restoration in 2017, the regional MEC is at a relatively high level, but the spatial distribution change is not obvious compared with 2014, which indicating that the stability of the ecosystem in the study area has gradually increased [43–45].

From Fig. 4, the MEC in the study area is normally distributed in different years overall. Before the earthquake, the MEC index was mainly between 1.3695 and 2.0214 g/cm², accounting for 68.28% of the sum total. After the Wenchuan earthquake in 2008, the MEC distribution curve shifted to the left as a whole, and the MEC index is mainly between 1.0926 and 1.8062 g/cm², accounting for 68.95% of the sum total. Therefore, regional eco-water conservation capacity decreased significantly at that time. After 3 y restoration, the MEC distribution curve moved to the right, and the MEC distribution was mainly between 1.1566 and 1.9276 g/cm², accounting 68.85% of the sum total. The eco-water conservation capacity was recovered greatly. By 2014, the MEC distribution curve still moved to the right. The MEC index was mainly distributed between 1.1932 and 1.9630 g/cm², accounting for 68.21%. The regional eco-water conservation capacity was further improved. In 2017, the MEC distribution curve moves slightly to the left, and the MEC index was distributed between 1.1793 and 1.9438 g/cm², accounting for 68.16%. The regional eco-water conservation

Table 2
Linear regression model and prediction

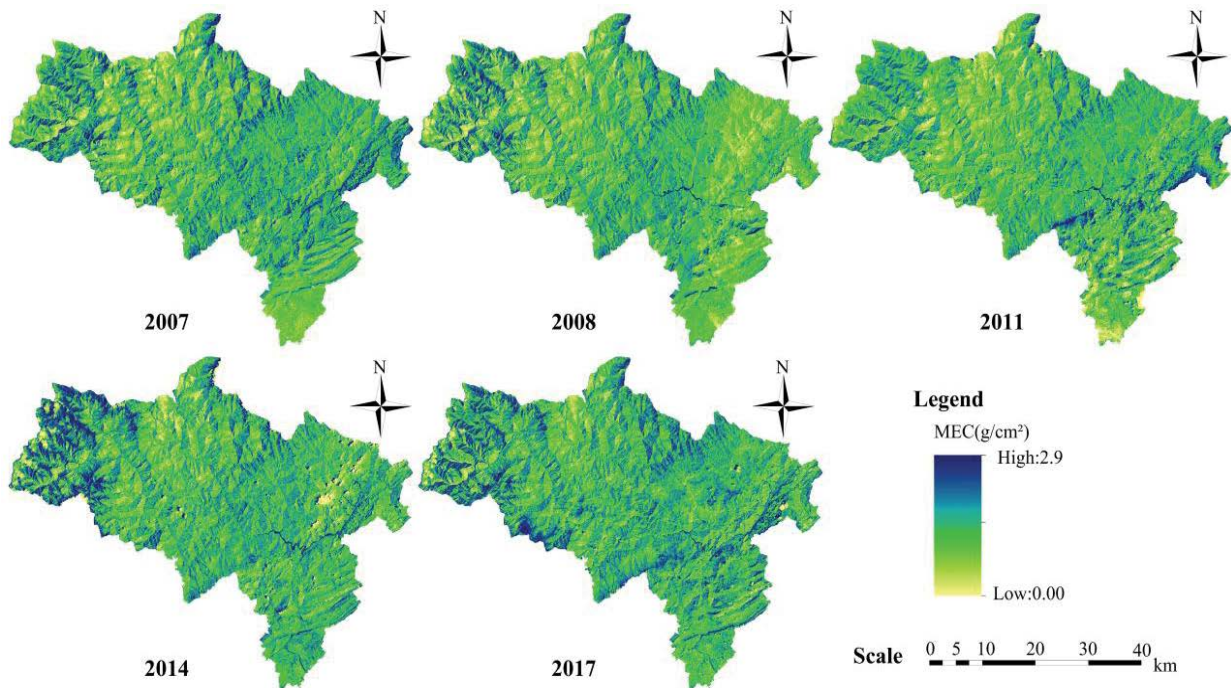| Number	Models of linear regression	Calibration		Prediction	
		r_c	$RMSE_c$	r_p	$RMSE_p$
1	$W_c = 6.5156 \times SMMRS - 3.3704$	0.914	0.012	0.911	0.089
2	$EWT_c = -0.216 \times MSI + 0.1593$	0.912	0.028	0.902	0.007

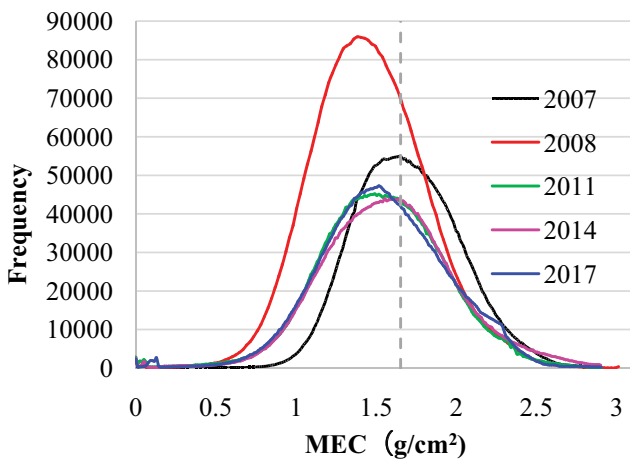Fig. 3. MEC spatial distribution of study area in 2007~2017.

Fig. 4. Histogram of MEC distribution of the study area in different years.

capacity decreased slightly. In general, the overall eco-water conservation capacity of the study area showed a sharp decline and then gradually increased. Compared with the previous stage, regional eco-water conservation capacity still declined during ecological restoration, which indicates significant effects on the regional ecological environment restoration. However, the stability of the ecological environment is relatively poor, and it is easily affected by human activities and natural disasters.

According to Eq. (8), QEC at any time was calculated and counted respectively in Table 3.

Table 3 shows that the total amount of eco-water conservation in the study area decreased and then increased gradually. Before the earthquake, the eco-water conservation in the study area was at the highest level, and it dropped 14.35% after the earthquake. With the promotion of ecological restoration, the amount of eco-water conservation increased continuously after the earthquake. By 2017, it had recovered to 48.8169 million tons. The increased amount of eco-water conservation was obvious in 2008, but the gap was still existed comparing with before. It shows that with the restoration of the ecological environment in the study area, the regional eco-water (layer) conservation capacity was increasing, but the increment was slowing down over time. The ecological water conservation capacity is difficult to recover to the level before the earthquake in a short time, so the ecological restoration in the stricken area requires continued attention.

3.3. Analysis on spatial change characteristics of eco-water conservation in the study area

3.3.1. Characteristics of eco-water conservation variation in different land use types

According to China's Second Land Survey data set, land use types in the study area was divided into cultivated land, forest land, garden land, grassland, bare land, construction land, and water area. According to the definition of eco-water (layer), water, and construction land was not included. In the study, there are 213.68 km² cultivated land, 2,550.78 km² forest land, 48.44 km² garden land, 51.97 km² grassland, and 103.80 km² bare land. Through the overlay analysis of GIS, Table 4 showed the average conservation modulus and its changes of different land types in different years.

From Table 4, the water conservation capacity of forest land is the strongest, followed by grassland, farmland,

Table 3
Statistics of QEC

Year	2007	2008	2011	2014	2017
QEC (10^4 t)	5,251.37	4,497.93	4,744.50	4,919.85	4,881.69
Rate of QEC change	–	–14.35%	1.83%	1.23%	–0.26%

Table 4
Average MEC and its changes of different land types in different years

Land types	2007		2008		2011		2014		2017	
	MEC	Rate of change	MEC	Rate of change	MEC	Rate of change	MEC	Rate of change	MEC	Rate of change
Cultivated land	1.594	–	1.395	–19.89%	1.391	–0.12%	1.538	4.89%	1.450	–2.92%
Forest land	1.722	–	1.481	–24.10%	1.562	2.68%	1.596	1.16%	1.612	0.53%
Garden land	1.576	–	1.334	–24.20%	1.394	1.97%	1.457	2.10%	1.407	–1.65%
Grass land	1.666	–	1.438	–22.78%	1.482	1.45%	1.57	2.95%	1.555	–0.49%
Bare land	1.524	–	1.321	–20.31%	1.423	3.40%	1.466	1.44%	1.368	–3.26%

garden land, and bare land. The forestland of the research area accounts for 82.73% of the total area. Because of strong eco-water conservation capacity of forestland, it occupies an absolute advantage from 2007 to 2017. The decline is of varying degree in eco-water conservation capacity of various land types after the earthquake. Among them, the reduction rate of MEC in woodland and garden land exceeds 24%, which is the main reason for the dramatically decline of regional ecological water conservation. By 2011, the MEC of most land types had increased. With an average annual growth rate of more than 2.5%, forestland and bare land was the most prominent land type among them, which have a connect relationship with vegetation restoration during that period. However, the conservation capacity of cultivated land declined slightly, which mainly because a large number of reclamation projects of damaged land were launched in the study area from 2009 to 2011. The action disturbed the arable layer in some degree, resulting in large fluctuation of MEC in cultivated land during that time. With the development of the ecological restoration in the stricken area, by 2014, eco-water conservation capacity of various land types has been further improved, the total amount of regional ecological water conservation has continued to approach the level before the earthquake. In particular, the start of agricultural activities caused the average annual MEC approaching 5% in cultivated land. Compared with 2014, the total amount of regional eco-water had a slight decline in 2017. However, the conservation capacity of forestland is still improving, which indicates that the stability of forestland ecosystem is better and the ecological recovery is stronger.

3.3.2. Characteristics of eco-water conservation variation in different land use types

According to the method of equal interval method, the slope of the study area was divided into 10 grades, the average MEC of each slope is calculated and collected in turn.

Table 5 showed the average MEC and annual change of different slopes in different years.

According to the method of equal interval method, the slope of the study area was divided into 10 grades, the average MEC of each slope is calculated and collected in turn. As shown in Table 5, MEC and slope are positively correlated with each other every year. Affected by diversified factors like earthquakes, secondary geological disasters, and human activities, ecological restoration is not synchronous in different regions, so the correlation varies in different years. It means that the ecological water conservation capacity of the study area is increasing with the growth of the slope. Interfered by various activities, the discrepancy of MEC in different slopes and years is apparent.

In light of the variation of MEC in every slope over time, the earthquake in 2008 and its secondary geological disasters resulted in massive destruction to vegetation, soil, and water body. The average MEC reduction rate in every slope of the study area was more than 12%, so the decrease is apparent. The decrease rate of MEC in the range of less than 25° is directly proportional to the change of terrain slope ($r = 0.97$, $p < 0.01$). The reduction rate of MEC gradually decreases with the increase of the slope ($r = 0.97$, $p < 0.01$) as slope is over 25°. There was the same situation from 2009 to 2011 when the average annual increase rate of MEC in every slope was more than 1%. From 2012 to 2014, the average MEC in each slope continued to increase, but the increase rate was apparent slow. Where the slope is less than 25°, the increase rate of average MEC was significantly higher than other areas. From 2015 to 2017, there was a certain difference in MEC change rate of every slope. The MEC in areas less than 20° declined slightly, the increase rate of MEC in other areas generally increased with the increase gradient of slope.

It means that topographic slope has an influence on eco-water conservation capacity, and its inflection point is around 25°. It primarily attributed to the area with slope

Table 5
Average MEC and annual change of different slopes in different years

Slopes (°)	2007		2008		2011		2014		2017	
	MEC	Rate of change	MEC	Rate of change	MEC	Rate of change	MEC	Rate of change	MEC	Rate of change
≤5°	1.640	–	1.431	–12.79%	1.475	1.03%	1.611	3.08%	1.555	–1.15%
5~10°	1.655	–	1.438	–13.14%	1.493	1.29%	1.600	2.36%	1.559	–0.84%
10~15°	1.677	–	1.444	–13.92%	1.519	1.73%	1.583	1.42%	1.566	–0.38%
15~20°	1.687	–	1.445	–14.37%	1.529	1.95%	1.571	0.90%	1.566	–0.09%
20~25°	1.690	–	1.446	–14.43%	1.531	1.95%	1.562	0.68%	1.568	0.12%
25~30°	1.693	–	1.449	–14.41%	1.532	1.91%	1.559	0.58%	1.571	0.26%
30~35°	1.698	–	1.457	–14.21%	1.534	1.76%	1.562	0.60%	1.577	0.32%
35~40°	1.706	–	1.469	–13.93%	1.541	1.63%	1.573	0.70%	1.587	0.29%
40~45°	1.723	–	1.490	–13.57%	1.557	1.49%	1.599	0.90%	1.603	0.09%
>45°	1.782	–	1.553	–12.87%	1.614	1.32%	1.670	1.16%	1.657	–0.27%

below 25° is mainly cultivated land and garden land, while the area with slope over 25° is mainly woodland and grassland. The earthquake and its secondary geological disasters changed many forestland, cultivated land moved into bare land. After the earthquake, the grass and shrubs in this area can cover the ground in a short time, which enhanced the improvement of ecological water conservation capacity. That's why the increase rate of MEC is higher than other areas as the slope is between 15° and 30° during 2009–2011. As the development of ecological restoration, cultivated land, and gardens in low slope areas were abandoned due to earthquakes (some even turned into bare land). After land rehabilitation and ecological restoration, agricultural activities resumed, the conservation capacity of regional MEC was significantly improved. In the area with a slope more than 25°, grass and shrubs recovered greatly from 2009 to 2011. However, the growth cycle of arbor forest is long, the soil in damaged forest is hard to recover under natural restoration in a short time, so the annual increase rate of MEC in high slope area is significantly lower than that in low slope area between 2012 and 2014. Low slope areas are the main place of human activity. Affected by many factors like agricultural activities and construction activities, MEC was fluctuated greatly. Coupled with the overall slow development of ecological restoration, MEC in low slope areas decreased slightly from 2015 to 2017.

3.3.3. Characteristics of eco-water conservation variation in different altitude

The altitude of the study area is varying from 540 to 4,769 m. According to the vertical distribution of regional vegetation and soil types, the altitude of the study area was divided into 10 grades by the method of equal interval method, then the average MEC in each altitude was calculated and collected in turn, shown in Table 6.

Table 6 shows that the correlation between eco-water conservation and altitude was not obvious every year. In general, the average MEC of the area below 3,000 m is higher, and that of 3,000–3,800 m is obviously lower. The MEC start increase again as the altitude is higher than 3,800 m.

The main reason for these characteristics and differences are closely related to the vertical distribution of soil and vegetation in the study area. The soil types below 3,000 m are mainly yellow soil, yellow–brown soil, and brown soil, the land types are mainly woodland, grassland, and arable land, so the water containment capability of soil and vegetation are higher than other study areas. Plants above 3,000 m are dominated by sub-alpine meadow soil and alpine meadow soil, while land types are mainly grassland and bare land, so the ecological water conservation capacity is weak. Study areas over 3,800 m are mainly covered by snow, so the MEC conservation capacity is also relatively high.

The MEC reduction rate in the study area after the earthquake is inversely proportional to the altitude ($r = 0.75$, $p < 0.05$). The MEC reduction rate in area below 1,800 m is over 14%, while the reduction rate in other area is about 12%, which indicates that the low-altitude areas were even strongly affected by Wenchuan earthquake. The main reason is that the regional seismic fault is located in the low-altitude region, the earthquakes and their secondary geological hazards are controlled by these seismic faults. The closer to the fault, the more frequent the geological hazards, and the greater the disturbance to the eco-water conservation capacity [24]. The MEC in different altitude was increased of varying degrees from 2009 to 2011. The average annual increase rate of MEC between 600 and 1,800 m is more than 2%. This indicates that under various ecological restoration measures, the regional eco-water conservation capacity has continued to increase and more artificial restoration measures have been taken in low altitude areas. Therefore, the promotion rate of this area is more apparent. The MEC in the whole area continued to increase from 2012 to 2014. The average annual increase rate of MEC in areas less than 600 m and areas between 1,800 and 3,400 m exceeds over the previous period. The main reason is that the area over 1,800 m is mainly restored by nature itself. Therefore, the capacity of eco-water conservation in this period was enhanced significantly. From 2014 to 2017, the difference in the annual average MEC variation of different altitude is obvious. Some areas have declined slightly, which indicating that the stability of the eco-water conservation capacity

Table 6
Average MEC and annual average change at different altitude in different years

Altitude (m)	2007		2008		2011		2014		2017	
	MEC	Rate of change	MEC	Rate of change	MEC	Rate of change	MEC	Rate of change	MEC	Rate of change
≤600	1.713	–	1.451	–15.31%	1.493	0.98%	1.623	2.88%	1.541	–1.67%
600~1,000	1.735	–	1.468	–15.35%	1.563	2.14%	1.572	0.20%	1.538	–0.71%
1,000~1,400	1.695	–	1.430	–15.63%	1.564	3.12%	1.592	0.58%	1.594	0.06%
1,400~1,800	1.626	–	1.391	–14.45%	1.484	2.24%	1.489	0.11%	1.573	1.88%
1,800~2,200	1.657	–	1.461	–11.83%	1.479	0.42%	1.597	2.64%	1.599	0.04%
2,200~2,600	1.810	–	1.603	–11.45%	1.632	0.61%	1.766	2.74%	1.724	–0.79%
2,600~3,000	1.850	–	1.621	–12.35%	1.679	1.20%	1.847	3.34%	1.830	–0.31%
3,000~3,400	1.582	–	1.383	–12.55%	1.473	2.17%	1.580	2.40%	1.523	–1.19%
3,400~3,800	1.497	–	1.295	–13.51%	1.365	1.80%	1.424	1.45%	1.380	–1.04%
>3,800	1.759	–	1.666	–5.28%	1.659	–0.13%	1.718	1.19%	1.740	0.41%

in these areas is poor and vulnerable responding to external interference.

4. Conclusion and discussion

Based on the research results of the research group for many years, this paper estimated the MEC and QEC in earthquake stricken areas during 2007 to 2017 by using optical remote sensing data and measured data, realized the dynamic monitoring of eco-water conservation in this area. Based on those facts, we can reach the following conclusions.

In terms of changes over time, the index of MEC and QEC before earthquake in the study area were largest (1.6964 g/cm² and 52.513 million tons), but it reached minimum after the earthquake in 2008 (1.4543 g/cm² and 44.793 million tons). In 2009–2017, the MEC and QEC were increasing gradually, but the change rate was decreasing over time. By September 2017, the average MEC and QEC in the study area recovered to 1.5481 g/cm² and 48.8169 million tons, respectively. This means that the ecological environment of the study area has been recovered through diversified ecological restoration measures after earthquake. Besides, the capacity of eco-water conservation was enhanced, but there was still a big gap compared with the capacity before the earthquake. In addition, the ecological restoration cycle is long, so the ecological environment needs further dynamic monitoring and scientific assessment.

In terms of spatial change, the characteristics of MEC spatial distribution are basically similar every year. The eco-water conservation capacity of the Jian River Basin, Duba River Basin, and the central and western edge areas was obviously high, but it was low in the southern, central northern area, and some market towns. Because of the fault dislocation during the earthquake, strong regional vibration ware generated, then more energy is released around the fault. That's, why the disturbance of MEC around the fault was more frequent than other parts of the study area.

The influence of Wenchuan earthquake on the eco-water conservation capacity varies from different land types, slopes, and altitudes. The area of the land forest in the study area is the largest (accounting 82.73% of the total area). The land forest is of highest conservation of those land types, but it was damaged severely, resulting the forest coverage decrement by 15.2%. This is a dominant factor that caused the 14.27% drop in MEC. Therefore, land types have the greatest impact on the eco-water conservation capacity. The distribution of MEC was positively correlated with slope change overall. The correlation was more than 0.8 ($p < 0.05$) except 2014. The main reason is that as the increases of the slope, the proportion of land with strong eco-water conservation capacity like forest land and grassland continues to increase. The Wenchuan earthquake and its secondary geological disasters caused a significant decrease in MEC at different slope. The most severely impact areas are with a slope of 15°–35°, where the reduction rate exceeded 14%. The correlation between eco-water conservation capacity and the altitude variation is not obvious in the study area. However, the average MEC in areas below 3,000 m is higher than areas over 3,000 m, which is related to the vertical distribution of soil and vegetation. The types of soil and vegetation are both important factors that affect the regional eco-water conservation capacity. Meanwhile, the eco-water conservation capacity of the area below 3,000 m faced more hazards in the earthquake, because the reduction rate of MEC was 31.85% higher than that above 3,000 m. This is closely related to the distribution of seismic fault.

Eco-water conservation capacity is of closely related to land types, slope, altitude, and fault distribution, so the formulation and adjustment of ecological restoration measures after disasters should take account these factors. Appropriate repair methods should be adopted according to the local condition. A distinction should be made between what is primary and what is secondary. If the slope is more than 25° and the altitude is over 1,800 m, natural restoration should be the principal method, and closing hillsides to facilitate afforestation should carried out appropriately. Areas with an altitude less than 1,800 m and a slope below 25° are mainly woodland and grassland, which should be restored by the method of combining artificial restoration with natural restoration. Areas along the fault zone, Minjiang River, Duba River, and other areas that are mainly cultivated land

and garden land should be considered using artificially restored methods.

Author contributions

MX: conceptualization, writing—original draft preparation, writing—review and editing, visualization, supervision, project administration, funding acquisition; JY: formal analysis, investigation; WY: validation; CW: resources; LD: data curation. All authors have read and agreed to the published version of the manuscript.

References

[1] W.N. Yang, J. Jian, Y.X. Li, Quantitative investigation of eco-water with remote sensing, J. Chengdu Univ. Technol., 2 (2008).

[2] W.N. Yang, Z.T. Qin, X. Yang, J. Jian, Y.X. Li, P.F. Pan, Novel quantitative measurement of eco-water layer based on quantitative remote sensing, J. Comput. Theor. Nanosci., 12 (2015) 2837–2841.

[3] J. Huang, W.N. Yang, X. Yang, B. Deng, The influence of eco-water retrieved by quantitative remote sensing on runoff in upper Minjiang River basin, Earth Sci. Res. J., 20 (2016) E1–E6.

[4] R. Stone, Wenchuan earthquake a Deeply Scarred Land, Science, 324 (2009) 713–714.

[5] Z.Y. Ni, Z.Y. Yang, W.L. Li, Y.B. Zhao, Z.W. He, Decreasing trend of geohazards induced by the 2008 Wenchuan earthquake inferred from time series NDVI data, Remote Sens., 11 (2019), doi: 10.3390/rs11192192.

[6] A.P. Yunus, X.M. Fan, X.L. Tang, D. Jie, Q. Xu, R.Q. Huang, Decadal vegetation succession from MODIS reveals the spatio-temporal evolution of post-seismic landsliding after the 2008 Wenchuan earthquake, Remote Sens. Environ., 236 (2020), doi: 10.1016/j.rse.2019.111476.

[7] H.C. Zeng, T. Lu, H. Jenkins, R.I. Negrón-Juárez, J.C. Xu, Assessing earthquake-induced tree mortality in temperate forest ecosystems: a case study from Wenchuan, China, Remote Sens., 8 (2016), doi: 10.3390/rs8030252.

[8] L.L. Liu, Q.Q. Shao, J.Y. Liu, C.J. Yang, Estimation of forest water conservation capacity in Qiongjiang River watershed, Ecol. Environ. Sci., 22 (2013) 451–457.

[9] J. Bustamante, D. Aragones, I. Afan, Effect of protection level in the hydroperiod of water bodies on Doñana's Aeolian Sands, Remote Sens., 8 (2016), doi: 10.3390/rs8100867.

[10] M. Falkenmark, J. Rockstrom, The new blue and green water paradigm: breaking new ground for water resources planning and management, J. Water Resour. Plann. Manage., 132 (2006) 129–132.

[11] M. Wigmosta, L. Vail, D. Lettenmaier, A distributed hydrology-vegetation model for complex terrain, Water Resour. Res., 30 (1994) 1665–1679.

[12] D.S. Chanasyk, E. Mapfumo, W. Williams, Quantification and simulation of surface runoff from fescue grassland watersheds, Agric. Water Manage., 59 (2003) 137–153.

[13] H. Langenberg, Hydrology: complex water future, Nat. Geosci., 5 (2012) 849–849.

[14] L.H. Xiong, L. Zeng, Impacts of introducing remote sensing soil moisture in calibrating a distributed hydrological model for streamflow simulation, Water, 11 (2019), doi: 10.3390/w11040666.

[15] S.N. Ni, J.L. Chen, C.R. Wilson, J. Li, X.G. Hu, R. Fu, Global terrestrial water storage changes and connections to ENSO events, Surv. Geophys., 39 (2018) 1–22.

[16] F. Zou, R. Tenzer, S.G. Jin, Water storage variations in Tibet from GRACE, ICESat, and hydrological data, Remote Sens., 11 (2019), doi: 10.3390/rs11091103.

[17] B. Mueller, M. Hirschi, S.I. Seneviratne, New diagnostic estimates of variations in terrestrial water storage based on ERA-Interim data, Hydrol. Process., 25 (2011) 996–1008.

[18] D.J. Cooper, J.S. Sanderson, D.I. Stannard, D.P. Groeneveld, Effects of long-term water table drawdown on evapo-transpiration and vegetation in an arid region phreatophyte community, J. Hydrol., 325 (2006) 21–34.

[19] C. Werner, M. Dubbert, Resolving rapid dynamics of soil-plant-atmosphere interactions, New Phytol., 210 (2016) 767–769.

[20] V. Shelia, J. Simunek, K. Boote, G. Hoogenboom, Coupling DSSAT and HYDRUS-1D for simulations of soil water dynamics in the soil-plant-atmosphere system, J. Hydrol. Hydromech., 66 (2018) 232–245.

[21] V. Levizzani, E. Cattani, Satellite remote sensing of precipitation and the terrestrial water cycle in a changing climate, Remote Sens., 11 (2019), doi: 10.3390/rs11192301.

[22] S.C. Mpala, A.S. Gagnon, M.G. Mansell, S.W. Hussey, The hydrology of sand rivers in Zimbabwe and the use of remote sensing to assess their level of saturation, Phys. Chem. Earth, 93 (2016) 24–36.

[23] J.G. Kerenyi, Application of remote sensing for the determination of water management parameters, Hungarian Meteorol. Serv., 122 (2018) 1–13.

[24] M.N. Sultana, M.S. Hossain, G.A. Latifar, Water quality assessment of Balu River, Dhaka Bangladesh, Water Conserv. Manage., 3 (2019) 08–10.

[25] A. Maqbool, W. Hui, M.T. Sarwar, Nanotechnology development for *in-situ* remediation of heavy metal (Loid)S contaminated soil, Environ. Ecosyst. Sci., 3 (2019) 09–11.

[26] A. Samsudin, M.A.A. Samah, M.Y. Ishak, Perception of government servants in Shah Alam on the utilization of food waste as a resource for biogas production in Malaysia, J. Clean WAS, 3 (2019) 16–20.

[27] R.Q. Huang, W.L. Li, Fault effect analysis of geo-hazard triggered by Wen-Chuan earthquake, J. Eng. Geol., 17 (2009) 19–28.

[28] N. Koizumi, S. Minote, T. Tanaka, A. Mori, T. Ajiki, T. Sato, H.A. Takahashi, N. Matsumoto, Hydrological changes after the 2016 Kumamoto earthquake, Japan, Earth Planets Space, 71 (2019), doi: 10.1186/s40623-019-1110-y.

[29] D. Jakovljevic, Z. Lozanov-Crvenkovic, Water quality changes after Kraljevo earthquake in 2010, Nat. Hazards, 79 (2015) 2033–2053.

[30] Y. Yamada, S. Kaga, Y. Kaga, K. Naiki, S. Watanabe, Changes of seawater quality in Ofunto Bay, Iwate, after the 2011 off the Pacific coast of Tohoku earthquake, J. Oceanogr., 73 (2017) 11–24.

[31] S. Uprety, P.Y. Hong, N. Sadik, B. Dangol, R. Adhikari, A. Jutla, J.L. Shisler, P. Degnan, T.H. Nguyen, The effect of the 2015 earthquake on the bacterial community compositions in water in Nepal, Front. Microbiol., 8 (2017), doi: 10.3389/fmicb.2017.02380.

[32] M.A. Khan, M.L. Sharma, Kachchh (India) earthquake 2001 - causes, severity and impact on groundwater resources, J. Environ. Sci., 15 (2003) 500–505.

[33] S.H. Lee, J.M. Lee, H. Yoon, Y. Kim, S. Hwang, K. Ha, Y. Kim, Groundwater impacts from the M5.8 earthquake in Korea as determined by integrated monitoring systems, Groundwater, 58 (2020) 951–961.

[34] K. Nakagawa, Z.Q. Yu, R. Berndtsson, T. Hosono, Temporal characteristics of groundwater chemistry affected by the 2016 Kumamoto earthquake using self-organizing maps, J. Hydrol., 582 (2020), doi: 10.1016/j.jhydrol.2019.124519.

[35] D. Parr, G.L. Wang, D. Bjerklie, Integrating remote sensing data on evapotranspiration and leaf area index with hydrological

modeling: impacts on model performance and future predictions, J. Hydrometeorol., 16 (2015) 2086–2100.

[36] G. Mendiguren, J. Koch, S. Stisen, Spatial pattern evaluation of a calibrated national hydrological model - a remote-sensing-based diagnostic approach, Hydrol. Earth Syst. Sci., 21 (2017) 5987–6005.

[37] C.M.M. Kittel, K. Nielsen, C. Tottrup, P. Bauer-Gottwein, Informing a hydrological model of the Ogooue with multi-mission remote sensing data, Hydrol. Earth Syst. Sci., 22 (2018) 1453–1472.

[38] J. Huang, W.N. Yang, L. Peng, M. Ashraf, Model of eco-water driving force affecting the evolvement of runoff in the upper Minjiang River Basin, Pol. Marit. Res., 23 (2016) 91–96.

[39] A.J. Richardson, C.L. Wiegand, Distinguishing vegetation from soil background information, Photogramm. Eng. Remote Sens., 43 (1977) 1541–1552.

[40] X.Y. Zhang, J.P. Li, Q.M. Qin, Y.J. Han, X.Y. Zhang, L.X. Wang, J.D. Guan, Comparison and application of several drought monitoring models in Ningxia, China, Trans. CSAE, 25 (2009) 18–23+317.

[41] X.J. Cheng, X.G. Xu, T.E. Chen, G.J. Yang, Z.H. Li, The new method monitoring crop water content based on nir-red spectrum feature space, Spectrosc. Spectral Anal., 34 (2014) 1542–1547.

[42] Q.M. Qin, L. You, Y. Zhao, S.H. Zhao, Y.J. Yao, Soil line automatic identification algorithm based on two-dimensional feature space, Trans. CSAE, 28 (2012) 167–171.

[43] P. Ceccato, S. Flasse, S. Tarantola, S. Jacquemoud, J. Gregoire, Detecting vegetation leaf water content using reflectance in the optical domain, Remote Sens. Environ., 77 (2001) 22–33.

[44] U. Hasan, M. Sawut, N. Kasim, N. Taxipulati, J.Z. Wang, I. Ablat, Hyperspectral estimation model of leaf water content in spring wheat based on grey relational analysis, Spectrosc. Spectral Anal., 38 (2018) 3905–3911.

[45] P.F. Pan, W.N. Yang, J. Jian, X.A. Dai, Remote sensing retrieval model of vegetation moisture content based on spectral index: a case study in Maoergai of Minjiang River upstream, Remote Sens. Inf., 28 (2013) 69–73.